Positronium collisions with rare-gas atoms: Free-electron gas plus orthogonalizing pseudopotential model

R. S. Wilde and I. I. Fabrikant

Phys. Rev. A **98**, 042703 — Published 17 October 2018

DOI: 10.1103/PhysRevA.98.042703

Positronium collisions with rare-gas atoms: Free electron gas plus orthogonalizing pseudopotential model

R. S. Wilde[1] and I. I. Fabrikant[2]

[1]*Department of Natural Sciences, Oregon Institute of Technology, Klamath Falls, Oregon 97601, USA*

[2]*Department of Physics and Astronomy, University of Nebraska, Lincoln, Nebraska 68588-0299, USA*

(Dated: September 25, 2018)

Abstract

Positronium collisions with rare-gas atoms are treated using the free-electron-gas approximation for exchange and correlation potential. The results confirm the absence of the Ramsauer-Townsend minimum in elastic scattering cross sections, but show lower cross sections in the lower-energy region when compared to previous pseudopotential calculations. This is explained by a more attractive *ab initio* correlation potential as compared to the previously used empirical potential. The results in the thermal energy region agree very well with most swarm measurements for all rare gas atoms. At higher energies the results are compared with beam experiments, and agreement for heavier rare gas atoms, Ar, Kr and Xe, is found to be very good. For He and Ne some discrepancies wth beam measurements are observed. This is explained by a poorer performance of the free electron gas potentials, based on the statistical Thomas-Fermi model, for systems with fewer electrons.

PACS numbers:

I. INTRODUCTION

Studies of positronium (Ps) collisions with atoms and molecules reveal interesting phenomena. In particular experiments of Laricchia *et al* [1–6] performed during the last eight years have shown that electron scattering and Ps scattering cross sections, when plotted as functions of the projectile velocity, are very similar for a variety of targets at energies above the Ps ionization or breakup threshold at 6.8 eV (v=0.5 a.u.). More recent experiments [5] on Ps scattering from Ar and Xe show a small cross section below the threshold which led to a speculation that there might be a Ramsauer-Townsend minimum in scattering of Ps from these rare-gas (Rg) atoms similar to that for electron scattering by heavy Rg atoms [7].

The similarity above the ionization threshold has been explained using the impulse approximation [8]. Calculations [9, 10] using a pseudopotential model have also been successful in reproducing the agreement above the threshold, but exhibit a larger cross section than experiment at lower velocities for the heavier rare-gas atoms. Other recent calculations in which the Ps-atom system is enclosed in a hard spherical wall have also led to larger cross sections below the ionization threshold for Rg atoms [11]. A number of other calculations [12–16] for Ps scattering by the Rg atoms have been done and these have been summarized in ref. [11]. These calculations all have resulted either in positive scattering lengths or in no indication of the Ramsauer-Townsend minimum. The Ramsauer-Townsend minimum usually occurs when the scattering length is negative, so that the s-wave scattering phase shift grows initially, then bends down due to a long-range attractive interaction and passes through 0 modulo π. This what happens in electron scattering by heavy Rg atoms: Ar, Kr, and Xe, and positron scattering from all Rg targets. However, because of the relative weakness of the van der Waals interaction compared to the polarization interaction, the scattering lengths for Ps scattering by these atoms is positive, and the Ramsauer-Townsend minimum does not occur for these targets [9]. Therefore, the overall picture of Ps-atom scattering is quite different from the electron scattering in the low-energy region. This is in stark contrast to the intermediate energy range from the Ps ionization threshold up to projectile velocities about 2 a.u. Here the Ps-A scattering is mostly controlled by the electron-atom exchange, which makes its cross section very similar to that for electron-atom scattering.

It appears that there is some discrepancy between experiment and theory for Ps scattering by Rg atoms below the ionization threshold. On the other hand, recent calculations

[11, 16] indicate that perhaps previous pseudopotential calculations [9] overestimate the Ps cross section in the low-energy energy region, and more calculations, incorporating more accurately exchange and correlations, are required.

A substantial deficiency of the pseudopotential calculations is that they do not include short-range correlation effects in an *ab initio* way. To account for the long-range correlation, the van der Waals potential with a short-range cut-off is usually introduced in the form

$$V_{corr} = -\frac{C_W}{R^6}[1 - \exp[-(R/R_c)^8]] \tag{1}$$

where C_W is the van der Waals constant, and R_c is an adjustable cut-off radius. While the long-range Ps-atom interaction is included properly in this way, the short-range correlations could be significantly underestimated. The total potential for the Ps-atom interaction might become therefore too repulsive, which would lead to a too rapid decrease of the scattering phase shifts at low energies.

In order to correct this deficiency, in the present paper we apply recently developed free electron gas (FEG) exchange and correlation energies [17] to calculate local scattering potentials for Ps collisions with Rg atoms. The FEG correlation potential is free of adjustable parameters and exhibits a strong attraction at short distances. We have previously used this model to investigate Ps-N_2 scattering [18] and were able to reproduce the resonance structure seen experimentally there and obtained good agreement with experiment above the ionization threshold, although again, at lower velocities the calculated cross sections seem to be substantially larger than the experimental.

Such local model exchange and correlation potentials have been used fairly extensively in electron-atom and electron-molecule scattering. One of the most common is the Hara free electron gas exchange potential (HFEGE) used first for e^--H_2 scattering [19]. The FEG model for the Ps-molecule scattering potential in refs. [17, 18] is similar to the HFEGE model except that there is an additional contribution to the exchange potential due to the positron interaction with the target electrons. The correlation potential of refs. [17, 18] is similar to the correlation potential for electron scattering derived by O'Connell and Lane [20].

These local approximations can take into account the attractive nature of the exchange potential [21] which occurs due to the Pauli exclusion principle and the creation of a Fermi hole [22, 23]. However, the local potentials cannot take into account the antisymmetric

character of the total wavefunction with respect to interchange of the projectile and target electrons. This feature is often incorporated by enforcing orthogonality between the scattering wave-function and the bound orbitals of the target atom or molecule. Morrison and Collins [24] have investigated the effect of enforcing orthogonality when using the HFEGE potential in electron-molecule scattering. In general it was found that enforcing orthogonality gave better agreement with exact static exchange calculations. Based on this result it might be expected that the orthogonality requirement should also have an effect on Ps scattering by atoms and molecules. In fact it was the main goal of refs. [9, 10] to model this orthogonality requirement through the use of a repulsive pseudopotential that is found by reproducing electron and positron scattering phase shifts.

Another method of enforcing orthogonality in electron or Ps scattering has been proposed by Mitroy *et al.* [25, 26] through the use of an orthogonalizing pseudopotential (OPP) first introduced by Krasnopolsky and Kukulin [27, 28]. In the present paper we develop the OPP for Ps scattering with Rg atoms and add it to our FEG exchange and correlation potentials. In this way we can attempt to take into account and study the effect of the Pauli principle on Ps-Rg scattering at low to intermediate velocities.

The rest of the paper is organized as follows. In Sec. II we briefly describe the FEG local and exchange potentials and derive an expression for the OPP. In Sec. III we present our results for the lighter rare gas atoms, He and Ne. In Sec. IV we present our results for the heavier rare-gas atoms Ar, Kr and Xe. Lastly, in Sec. V, we present our conclusions and outlook. Atomic units are used throughout unless stated otherwise. As it has become customary since the discovery [1] of similarities between electron and Ps scattering, in most cases we present the Ps scattering cross sections as functions of velocity rather than energy, although in the thermal energy region we will also use the energy scale.

II. POTENTIALS

In this section we describe the theory for calculation of the exchange and correlation potentials using the FEG method of [17] and the inclusion of orthogonality using the OPP. The FEG potentials are local, but the OPP is non-local. To obtain the radial equations for the Ps center of mass motion, we write the total Ps wave-function in the form

$$\Psi(\mathbf{r}_e, \mathbf{r}_p) = G(\mathbf{R})\psi(\mathbf{t}) \tag{2}$$

where the Ps center of mass is related to the positron and electron coordinates by $\mathbf{R} = (\mathbf{r}_e + \mathbf{r}_p)/2$ and we define the relative coordinate as $\mathbf{t} = \mathbf{r}_e - \mathbf{r}_p$.

When the Schrödinger equation governing the Ps + atom collision is averaged over the ground state Ps function, given by

$$\psi(\mathbf{t}) = \frac{1}{\sqrt{8\pi}} e^{-t/2}, \tag{3}$$

the static potential vanishes and we obtain the equations for the function $G(\mathbf{R})$ that describe the Ps center of mass motion

$$[\nabla_R^2 + p^2] G(\mathbf{R}) = 4V_{XC}(R)G(\mathbf{R}) + 4\gamma\hat{P}G(\mathbf{R}) \tag{4}$$

where V_{XC} is the local exchange plus correlation potential derived in [18], and $\gamma\hat{P}$ is an orthogonalizing pseudopotential as defined in [14, 15, 26]. In the remainder of this section we describe the FEG local exchange and correlation potentials and derive the expression for the OPP kernel.

A. FEG exchange and correlation potentials

In the FEG method the exchange and correlation energies are functions of the Fermi momentum k_F. The dependence on position is given by the Thomas-Fermi relation in which the Fermi momentum depends on the target charge density $\rho(\mathbf{r})$,

$$k_F(\mathbf{r}) = [3\pi^2\rho(\mathbf{r})]^{1/3}. \tag{5}$$

As described in ref. [17] we evaluate k_F at the center of mass of the Ps atom so that $\mathbf{r} = \mathbf{R}$. The exchange and correlation potentials are then summed to give the total local approximation to the scattering potential. To calculate the charge densities we have used, for all rare-gas atoms except Helium, the Hartree-Fock wave functions of Mann [29]. For He we have used the two parameter wave function of Green *et al.* [30] that closely approximates the Hartree-Fock wave function.

In order to take into account the long range behavior of the correlation potential we have used the long range form

$$V_W(R) = -\frac{C_W}{(R^2 + R_c^2)^3} \tag{6}$$

where the cutoff parameter R_c is adjusted to match smoothly to the FEG correlation potential below some transition radius R_t at a scattering velocity of v=0.01 a.u. For He we have used R_c=1.65 a.u which gives R_t=1.95 a.u. For all other atoms we have chosen R_c = 1.3 a.u. which gives R_t = 2.72 a.u. for Ne, 3.09 a.u. for Ar, 3.27 a.u. for Kr and 3.36 a.u. for Xe. The values of C_W used in the present calculations are for He 13.37 a.u. [15]. For Ne, Ar, Kr, Xe the values are 26.48, 98.69, 146.71 and 227.38 a.u., respectively [31]. These values are the same as those used by Swann and Gribakin [11].

Another common method of including correlation is by using the empirical potential (1) with an adjustable cut-off radius R_c. This form has been used in the pseudopotential calculations for various targets of refs. [9, 10] as well as the calculations of Swann and Gribakin for Rg targets [11].

In Fig. 1 we show the absolute value of the exchange and correlation potentials for each atom at a Ps velocity of 0.01 a.u. The potentials depend very weakly on the Ps velocity. Due to the rapid rise of the charge density as $r \to 0$ the strength of the potential increases rapidly in this region.

An interesting feature of the exchange plus correlation potential is that at intermediate values of R it becomes repulsive. This is shown in Fig. 2. This is due to the exchange energy becoming positive for small k_F, see ref. [17]. Due to this effect the potential does not reach its asymptotic form until relatively large values of R. It should be noted that, although the total potential becomes repulsive for a small range of intermediate values of R, it eventually becomes attractive again. The value of R at which the potential becomes attractive again increases as the size of the atom increases. For He and Ne this transition occurs at the relatively small distances of 2.83 a.u. and 3.53 a.u., respectively. For the larger atoms Ar, Kr and Xe the transition occurs at the larger distances of 4.61 a.u., 5.07 a.u. and 5.77 a.u., respectively.

B. Orthogonalizing Pseudopotential OPP

As mentioned above we use the OPP to enforce orthogonality between the electron in Ps and the occupied target atom orbitals, ϕ_{nlm}. The OPP is defined by the projection operator

[26]

$$\gamma\hat{P} = \gamma\delta(\mathbf{r}_p - \mathbf{r}'_p)\sum_i^N |\phi_i\rangle\langle\phi_i|. \tag{7}$$

which is added to the exchange and correlation potentials V_{XC} and leads to the non-local term. The delta function ensures that the OPP affects only the electron coordinate emphasizing in this way the dominant role of the electron constituent of Ps in the scattering. The strength parameter γ in these equations is made large enough so that orthogonality is enforced and the scattering calculations are converged in the sense that further increase of γ leads to a negligible change in the phase shifts and cross sections. The sum is over the N occupied orbitals of the target atom.

For simplicity we derive the OPP kernel $K(\mathbf{R}, \mathbf{R}')$ for He, the generalization to the heavier Rg atoms is then relatively straightforward. For He the OPP of (7) includes only one term due to the occupied $1s$ orbital and the non-local term in (4) is given by

$$\int K(\mathbf{R}, \mathbf{R}')G(\mathbf{R}')d^3R' = \int\int \psi^*(\mathbf{t})\phi_{1s}(\mathbf{r}_e)\phi^*_{1s}(\mathbf{r}'_e)\psi(\mathbf{t}')G(\mathbf{R}')d^3t'd^3r'_e. \tag{8}$$

In order to facilitate evaluation of the integrals in Eq. (8), we change coordinates from $(\mathbf{r}'_e, \mathbf{t}')$ to $(\mathbf{r}_p, \mathbf{R}')$ which is similar to that used by Fraser [32, 33]. The Jacobian of this transformation equals 64. This follows from the relations

$$\mathbf{t} = 2(\mathbf{R} - \mathbf{r}_p); \quad \mathbf{t}' = 2(\mathbf{R}' - \mathbf{r}_p) \tag{9}$$

and

$$\mathbf{r}_e = 2\mathbf{R} - \mathbf{r}_p; \quad \mathbf{r}'_e = 2\mathbf{R}' - \mathbf{r}_p. \tag{10}$$

Furthermore we make the expansions

$$\psi^*(2|\mathbf{R} - \mathbf{r}_p|)\phi_{1s}(|2\mathbf{R} - \mathbf{r}_p|) = \sum_l \frac{(2l+1)}{4\pi} A_l(R, r_p)P_l(\cos\theta_{Rr_p}) \tag{11}$$

and

$$\phi^*_{1s}(|2\mathbf{R}' - \mathbf{r}_p|)\psi(2|\mathbf{R}' - \mathbf{r}_p|) = \sum_{l'} \frac{(2l'+1)}{4\pi} A^*_{l'}(R', r_p)P_{l'}(\cos\theta_{R'r_p}). \tag{12}$$

The coefficients $A_l(R, r_p)$ are calculated numerically as suggested by Fraser [32, 33]. From Eq. (8) we obtain

$$\int K(\mathbf{R}, \mathbf{R}')G(\mathbf{R}')d^3R = 64\gamma\sum_{ll'}\int\int \frac{(2l+1)(2l'+1)}{(4\pi)^2} A_l(R, r_p)A^*_{l'}(R', r_p) \times P_l(\cos\theta_{Rr_p})P_{l'}(\cos\theta_{R'r_p})G(\mathbf{R}')d\mathbf{r}_p d\mathbf{R}'. \tag{13}$$

Now we use the spherical harmonic addition theorem, perform the angular integration over $\mathbf{r}_p$ and make the partial wave expansion

$$G(\mathbf{R}) = \sum_{LM} \frac{F_L(R)}{R} Y_{LM}(\hat{R}) \tag{14}$$

to obtain the radial equations

$$\left[\frac{d^2}{dR^2} - \frac{L(L+1)}{r^2} + p^2\right] F_L(R) = 4V_{XC}(R)F_L(R) + 4\gamma \int K_L(R,R')F_L(R')dR' \tag{15}$$

where V_{XC} is the local exhange plus correlation potential and the L-dependent kernel is given by

$$K_L(R,R') = 64RR' \int A_L(R,r_p)A_L^*(R',r_p)r_p^2 dr_p. \tag{16}$$

In the case of an atom with more than one occupied orbital we must evaluate the sum over the occupied orbitals of the target atom. Each orbital may be written as

$$\phi_{nlm}(\mathbf{r}) = R_{nl}(r)Y_{lm}(\hat{r}). \tag{17}$$

We may now obtain a radial equation like that of (15). Noting that $\theta_{\mathbf{rr}'} = \theta_{\mathbf{RR}'}$ and using properties of the spherical harmonics and the Wigner 3-j symbols we obtain for the L-dependent kernel

$$K_L(R,R') = 64RR' \sum_{nll'} C_{ll'L} \int A_{nll'}(R,r_p)A_{nll'}(R',r_p)r_p^2 dr_p. \tag{18}$$

where $A_{nll'}$ is the Legendre expansion coefficient in

$$\psi(2|\mathbf{R}-\mathbf{r}_p|)R_{nl}(|2\mathbf{R}-\mathbf{r}_p|) = \sum_{l'} \frac{(2l'+1)}{4\pi} A_{nll'}(R,r_p)P_{l'}(cos\theta_{Rr_p}) \tag{19}$$

and

$$C_{ll'L} = \frac{(2l+1)(2l'+1)}{4\pi} \begin{pmatrix} l & l' & L \\ 0 & 0 & 0 \end{pmatrix}^2. \tag{20}$$

The radial equations (15) are solved iteratively. The phase shifts and cross sections are converged for values of $\gamma > 3$ a.u. We have used $\gamma = 20$ a.u. in all calculations. We also note that the OPP acts as a repulsive potential that forces the wave function to be small at small values of R for all values of L. This is unlike the electron-atom scattering case where the orthogonality affects only the symmetries corresponding to the occupied atomic orbitals.

III. PS SCATTERING BY HE AND NE

In this section we consider scattering of Ps by the lighter Rg atoms, He and Ne.

In Fig. 3 we show the phase shifts for Ps scattering by He and Ne using the FEG exchange and correlation potentials with and without inclusion of the OPP. Without the OPP the scattering exhibits a low energy resonance, in P wave for He and in D wave for Ne. When the effect of orthogonality is included by adding the OPP to the FEG potentials the resonance disappears due to the repulsive nature of the OPP.

In Fig. 4 we show the cross sections for elastic scattering of Ps by He and Ne using our FEG exchange and correlation potentials with and without the OPP as well just the exchange potential with the OPP, but without correlations. The cross section near zero velocity is only slightly larger than the results of [11], but is a fair amount larger than the experimental results above the ionization threshold. Note that after adding of Ps ionization cross sections to the elastic cross sections, the disagreement with the experiment would become even worse, although the ionization cross sections for these targets (with peak values 1.5×10^{-16} and 3×10^{-16} cm^2 for He and Ne respectively [35]) are not large.

In Fig. 5 we show the phase shifts for Ps-He and Ps-Ne scattering at velocities below the ionization threshold and compare the present results with the calculations of Swann and Gribakin [11] and, for He, with the calculations of Barker and Bransden [36]. In this calculation we have used the correlation potential of Eq. (1) with $R_c = 2.5$ a.u. which has also been used in the calculations of Swann and Gribakin [11]. Our phase shifts decrease more rapidly than those from other calculations, and this leads to a larger scattering cross section at velocities near 0.5 a.u. It appears that the OPP overestimates the repulsive effect of orthogonality for these lighter target atoms at intermediate velocities. It could be also possible that our local exchange potential, based on the statistical Thomas-Fermi model, is too approximate for atoms with a few electrons, like He and Ne, and underestimate the effective attraction due to exchange.

When solving the radial equations (15) at low Ps velocities ($v < 0.1$ a.u.) we have often encountered some instability in the S-wave phase shift due to the large non-local OPP term. In order to extrapolate the S-wave phase shift to low velocities we attempted to use the modified effective range expansion [9, 37–39] for the phase shift

$$\tan \delta_0 = -Ap - r_0 A^2 p^3/2 + \pi\gamma^4 p^4/15 + 4A\gamma^4 p^5 \ln|2pd|/15 + O(p^5), \qquad (21)$$

where $p = 2v$ is the Ps center of mass momentum, A is the scattering length, r_0 and d are other parameters depending on the short-range interaction, and

$$\gamma^4 = 2mC_W, \qquad m = 2 \text{ a.u.}$$

It is well known, however, that for long-range potentials δ_l as a function of p is nonanalytical at $p = 0$ [37]. (This explains the logarithmic term in expansion (21)). Moreover, this expansion has a very small (if not zero) convergence radius, therefore inclusion of higher-order terms there leads to a spurious behavior of $\delta_l(p)$. This is particular relevant when the parameter γ^4 is large, like in the case of Xe when it equals 920 a.u. In this case the p^4 terms becomes larger in absolute magnitude than the p^3 term already at $p = 0.17$ a.u. ($E = 0.2$ eV). A more reasonable approach would be to expand $\delta_l(p)$ about the point where this function is analytical. Assuming that this point is close to the origin and reexpanding δ_0 again in powers of p, we obtain the following polynomial extrapolation formula

$$\delta_0 = -Ap + Bp^3 + Cp^4 + Dp^5, \tag{22}$$

where all coefficients are treated as fit parameters. We could have included the term p^2 as well, but Eq. (21) suggests that this term is insignificant. Calculations for all rare gas atoms show that indeed Eq. (22) works much better for extrapolation to lower p than Eq. (21). The fit parameters and cross section at v=0 for He and Ne are shown in Table I. For comparison we also show results of previous calculations and experiments for the scattering length and cross section at v=0 in Table II.

Using the present FEG model for the correlation potential we obtain the scattering lengths of 1.77 a.u. and 1.87 a.u. for He and Ne, respectively. These are in quite good agreement with the many body theory values, 1.70 a.u. for He and 1.76 a.u. for Ne, of Green et al. [16]. They are slightly larger than the recommended values of ref. [11], 1.60 for He and 1.65 for Ne. When correlation is neglected we obtain the scattering lengths of 1.87 a.u. and 2.08 a.u. for He and Ne respectively. These are also in good agreement with the frozen target values, 1.86 a.u. for He and 2.02 a.u. for Ne, of ref. [11].

Mitroy and Ivanov [14] have employed the OPP in low velocity calculations for Ps scattering with several closed shell atoms. Using the stochastic variational method, they obtained frozen target scattering lengths of 1.84 a.u. for He and 2.02 a.u. for Ne. These compare well with the present results of 1.87 a.u. for He and 2.08 a.u. for Ne. When the van der Waals

interaction is included the stochastic variational method results in scattering lengths of 1.57 a.u. for He and 1.55 a.u. for Ne. These are somewhat smaller than the present values of 1.77 a.u. for He and 1.87 a.u. for Ne. This difference may be attributed to the fact that Mitroy and Ivanov use a different model for the van der Waals interaction.

In Fig. 6 we show the momentum transfer cross sections for Ps scattering by He and Ne compared with the many body theory calculations of [16] and various experimental swarm measurements. These are based on observation of Ps thermalization in a gas environment and describe the Ps-Rg interaction at thermal energies. For He the earlier results of Nagashima *et al.* [54, 55] are in much better agreement with the theory than those of Skalsey *et al.* [56]. More recently Engbrecht *et al.* [57] attempted to determine the energy dependence of the momentum transfer cross section in the region between 0 and 0.8 eV from measurements of Ps energy as a function of time. The shape of their curve is consistent with the theoretical results. However, the absolute magnitude of the cross section is even lower than that of Skalsey *et al.* To resolve this controversial situation, experimental results in the energy (velocity) range joining the regions of beam and swarm measurements are certainly warranted. For Ne both swarm measurements agree with the theory, but again, measurements in the gap corresponding to the velocity range between 0.2 and 0.5 a.u. (1 to 7 eV) would be beneficial.

IV. PS SCATTERING BY AR, KR AND XE

In Fig. 7 we show the phase shifts for Ps scattering by Ar and Xe using the FEG exchange and correlation potentials with and without inclusion of the OPP. Again, without the OPP the scattering exhibits a low energy resonance, in P wave for Ar and in D wave for Xe. For Xe there is also an F-wave resonance that is prominent at low velocities. When the effect of orthogonality is included by adding the OPP to the FEG potentials, the resonances again disappear due to the repulsive nature of the OPP.

In Fig. 8 we show the cross sections for Ps scattering by Ar and Xe compared with experimental measurements and the calculations of [11]. In the present calculations we use the OPP potential with the FEG exchange potential and with either no correlation, FEG correlation or the correlation potential with cutoff of Eq. (1). We have also added the ionization cross sections above the ionization threshold to the FEG exchange and correlation

plus OPP cross section using the binary encounter approximation of [10] to obtain the total scattering cross section. The present total cross sections above the ionization threshold are slightly larger than the experimental results and previous pseudopotential calculations of [10]. However, at velocities below the ionization threshold the present cross sections are quite different from the pseudopotential results. The pseudopotential results [9] exhibit a peak in the cross section in this region whereas the present calculations do not. This peak was explained [9] by a rapid decrease of the S-wave and the P-wave phase shifts in the low-velocity region. Looking at the present results for the phase shifts, we conclude that the pseudopotential calculations either overestimated the Pauli repulsion or underestimated the attraction due to short-range correlations, or both.

In Fig. 9 we show the phase shifts for Ar and Xe at velocities below the ionization threshold using the correlation potential of Eq. (1) with a cutoff radius of R_c=2.5 a.u. for Argon and R_c= 3.0 for Xenon. The present phase shifts are a fair amount larger than the previous pseudopotential calculations which indicates that the overall FEG exchange, correlation and OPP is more attractive than the pseudopotential. This might be expected since the pseudopotentials of refs. [9, 10] are determined by fitting to electron and positron static-exchange scattering phase shifts, therefore the only attractive potential included is the empirical correlation potential of (1) which is much weaker at small R than the FEG correlation potential.

Therefore it is interesting to compare the FEG correlation potential with the form of Eq. (1). In Fig. 10 we compare the FEG correlation potentials with the potential of Eq. (1) with R_c=2.5 a.u. for Ar and R_c=3.0 a.u. for Xe. At small values of R the FEG potential becomes very strongly attractive while the correlation potential of Eq. (1) goes to zero. However, at small values of R the short range repulsion of the OPP masks the attractive effect of the exchange and correlation potentials. At intermediate values of R, however, the potential of Eq. (1) is slightly more attractive than the FEG correlation potential. This leads to a smaller cross section at low velocities and, in the case of Xe, to a Ramsauer-Townsend minimum.

In general we see relatively good agreement with experiment for the heavier rare-gas atoms both above and below the ionization threshold when using the FEG exchange and correlation potentials plus the OPP. The worse agreement for the lighter atoms, He and Ne, may be due to the FEG model being not as appropriate for systems with fewer electrons.

In Fig. 11 we present our cross section and phase shifts for scattering of Ps by Kr. We obtain similar results to that of Ar and Xe.

As we did for He and Ne, we have fit the low velocity S-wave phase shift to the polynomial expansion of Eq. (22), and we present the fit parameters for Ar, Kr and Xe in Table III. For comparison we also show results of previous calculations and experiments for the scattering length and cross section at v=0 in Table IV. When using the FEG potentials plus OPP, we have obtained the scattering lengths of 1.95 a.u. for Ar, 1.98 a.u. for Kr and 1.86 a.u. for Xe. The recommended values of [11] are 2.0 a.u. for Ar, 2.3 a.u. for Kr and 2.6 a.u. for Xe. The recommended values are becoming larger with the size of the atom whereas our FEG plus OPP results are quite close to one another, and in fact the result for Xe is smaller than Ar and Kr. The scattering lengths from the stochastic variational method including the van der Waals interaction method are 1.79 a.u. for Ar [14], 1.98 a.u. for Kr and 2.29 a.u. for Xe [15] which are also somewhat smaller than the recommended values of [11].

Our present scattering lengths without including correlation are 2.60 a.u. for Ar, 2.84 a.u. for Kr and 3.16 a.u. for Xe which may be compared with the frozen target calculations of [11], 2.81 a.u. for Ar, 3.11 a.u. for Kr and 3.65 a.u. for Xe. In both cases the scattering lengths are increasing with the size of the atom, but the present results are somewhat smaller than the frozen target results. The frozen target stochastic variational phase shifts are 2.85 a.u. for Ar, 3.18 a.u. for Kr and 3.82 a.u. for Xe which are again larger than the present results. The difference here might be due to the effect of the strongly attractive FEG exchange potential in the present calculations.

Recently Shibuya and Saito [58] have proposed a method to convert measured Ps annihilation rates into total and partial Ps scattering cross sections in the Ps energy range 0-80 meV. They applied this method to Ps-Xe scattering and obtained scattering phase shifts at thermal energies shown in Fig. 12. Their scattering length is 2.06 a.u. for Xe which is quite close to our present value of 1.86 a.u. Based on this result, they claim that "the positron plays the more important role during Ps-Xe collisions in the ultralow-energy region. This differs from the understanding that electron exchange plays the dominant role in the intermediate-energy region". We agree that the low-energy scattering is controlled by a repulsive potential, but as we see through the use of the OPP, the repulsion is due to the effect of orthogonality between the electron in Ps and the electrons in the atomic target, so the scattering is still controlled mostly by electron exchange, although the cross section

is quite different from that of e^--Xe because of different long-range interactions in the two processes.

By extrapolation to higher Ps energies, Shibuya and Saito have also found a peak in the total Ps-Xe cross section near 0.4 eV that has a very large magnitude of (430 ± 100) 10^{-16} cm^2. This peak is significantly higher than that obtained in our previous pseudopotential calculations [10] and that found by Blackwood *et al.* [12]. We also note that the result of [12] was later found to be in error due to a numerical inaccuracy [59] and there is, in fact, no peak. The cross section of Shibuya and Saito in the $E = 1$ eV region is also much higher than that obtained in beam measurements [5]. In particular these measurements give the cross section 9×10^{-16} cm^2 at $E = 1.7$ eV whereas Shibuya and Saito obtain 200×10^{-16} cm^2 at $E = 1$ eV. Such a striking disagreement can be, at least at large extent, explained by the extrapolation procedure used by Shibuya and Saito. They use the effective range theory expansion, Eq. (21), for δ_0 and similar expansions for δ_1 and δ_2 [37]. As was discussed in Sec. III, these expansions are very badly divergent already for $E = 0.2$ eV, even with $\gamma^4 = 460$ a.u. in Eq. (22), used by Shibuya and Saito, instead of actual $\gamma^4 = 920$ a.u. for Xe. The parameters of Shibuya and Saito produce for partial cross sections at $E = 0.4$ eV ($v = 0.12$ a.u.) $\sigma_1 = 162 \times 10^{-16}$ cm^2 and $\sigma_2 = 249 \times 10^{-16}$ cm^2 leading to the total cross section exceeding 400×10^{-16} cm^2 which is not supported by any theory.

In our present calculations using FEG exchange and correlation potentials plus the OPP we actually see a minimum in the Ps scattering cross section at low energies (velocities). To understand this we show in Fig. 12 the present phase shifts for Ps-Xe scattering compared with the results of Shibuya and Saito [58] and our previous pseudopotential results [10] for Ps energies of 0-80 meV. Our present S-wave phase shift decreases the most slowly of the three and our P-wave phase shift is quite negligible at these ultra-low energies. In fact the present P-wave phase shift is slightly positive in the thermal energy range, and becomes negative at a Ps energy of 256 meV. This means that the P-wave phase shift is very small in the low energy region and the slowly decreasing S-wave phase shift is dominant which leads to a minimum in the cross section before the P-wave and other higher partial waves begin to grow and the cross section starts to increase at higher velocities. Our present results seem more consistent with the beam measurements, but once again we see that further measurements in the 0.2-0.5 a.u. (E=1 to 7 eV) range are warranted.

We also see from Table III that the scattering length is very sensitive to the correlation

potential. In fact, when using the empirical correlation potential of Eq. (1) with $R_c = 3.0$ a.u. for Xe, we obtain a negative scattering length indicating the presence of a Ramsauer-Townsend minimum. However, calculations with a more reliable correlation potential, the measurements of Shibuya and Saito, and all other calculations of Ps-Xe scattering suggest that the existence of the Ramsauer-Townsend minimum in Ps-Xe scattering is highly unlikely.

In Fig. 13 we show the momentum transfer cross sections for the heavier Rg atoms Ar, Kr and Xe using the FEG exchange and correlation potentials with the OPP. We also show the calculations of Swann and Gribakin [11] using Eq. (1) with two different values of cutoff radius, R_c. For Ar these values are $R_c = 2.5$ and 3.0 a.u. and our present cross section lies between these. For Kr and Xe the cutoff radii are larger, R_c=3.0 and 3.5 a.u. and our cross sections are smaller than the calculations of [11]. Since a larger cutoff radius leads to a weaker correlation potential, this seems to indicate that the Ps-Rg interaction in our case is effectively more attractive than that of Swann and Gribakin.

For Ar the experimental results are quite varied, but we obtain relatively good agreement, while for Xe our momentum transfer cross section is in excellent agreement with the measurement of Shibuya *et al.* [61].

Lastly, in Fig. 14 we compare our Ps scattering cross sections with electron scattering cross sections for the heavier rare gas atoms Ar, Kr and Xe. We see a strong similarity between the electron and Ps total cross sections above the ionization threshold confirming observations [1–4, 6]. Below the threshold the Ps cross sections are larger but exhibit a minimum like the electron cross sections. This minimum is different in nature: in Ps scattering it is due to the slow decrease of the S-wave phase shift at low Ps velocities, while for electron scattering it is a Ramsauer-Townsend minimum.

V. CONCLUSION AND OUTLOOK

We have applied the exchange and correlation energies of Ps in a free electron gas [17] to construct local exchange and correlation potentials describing Ps-atom interaction. To take into account the effect of antisymmetry of the total wavefunction with respect to interchange of the Ps electron and the target electron, we can impose the orthogonality of the Ps electron orbital to the occupied orbitals of the target atom. In order to model the effect

of orthogonality we have added an orthogonalizing pseudopotential (OPP) [25–28] which leads to a short range, non-local repulsive potential. The constructed potentials were then used to calculate phase shifts and cross sections for Ps scattering by Rg atoms at low to intermediate Ps velocities.

The use of just the attractive local potentials leads to shape resonances at low Ps velocities that are not seen experimentally. The addition of the OPP to the local potentials removes the resonances and generally leads to good agreement with beam experiments [1, 5, 34], especially for the heavier atoms Ar, Kr and Xe. For He and Ne the cross sections are too large compared with experiment in the low-energy region which may be due to the FEG potential not being as appropriate for such smaller systems since it is based on the statistical Thomas-Fermi model.

At velocities below the ionization threshold the cross section is very sensitive to the intermediate and long range correlation potential. This is because the exchange and correlation potentials are masked by the OPP at small values of R. In fact for Xe we can get a Ramsauer-Townsend type minimum in the cross section if the correlation potential is attractive enough in the region of intermediate R. This sensitivity illustrates the necessity of accurate determination of the exchange and correlation potentials in this region.

The use of the local FEG exchange and correlation potentials with the OPP, in general leads to smaller cross sections and better agreement with results of beam measurements than previous pseudopotential calculations. In the thermal energy region, inaccessible to beam experiments, our results are compared with swarm experiments measuring the Ps momentum transfer cross sections from observation of Ps moderation in gases. An excellent agreement with measurements of Nagashima *et al.* [54, 55] for He, Ne, and Ar, with Skalsey *et al.* [56] for Ne, and with Shibuya *et al.* [58, 61] for Xe, has been obtained. However, the extrapolation of the Ps-Xe phase shifts, obtained by Shibuya and Saito [58] to higher energies leads to strongly overestimated (by an order of magnitude) total cross sections. This is due to the failure of the effective range expansion, Eq (21), at higher energies.

We conclude that our model provides a good description of Ps scattering by Rg atoms, especially the heavier atoms Ar, Kr and Xe. Our calculations confirm the positive sign of the scattering length and the absence of the Ramsauer-Townsend minimum in Ps scattering by heavier rare-gas atoms. However, the S- and P-wave scattering phase shifts decrease with energy significantly slower than in the previous pseudopotential calculations. This leads to

a minimum, albeit of not Ramsauer-Townsend type, in the cross section as a function of energy and significantly improves agreement with the beam experiments in the energy range below the Ps ionization threshold.

The next important step would be a generalization of the present model to Ps-molecule scattering. A particular interesting case is Ps-N_2 resonant scattering treated in [18] without incorporation of the OPP. Since there is no occupied π_g orbital in N_2, inclusion of OPP should not affect the Π_g resonance in e-N_2 scattering. However, Ps-N_2 scattering is different since electron partial waves there are mixed. Therefore the OPP in this problem can contribute noticeably.

Acknowledgments

The authors are grateful to G. Laricchia for stimulating discussions, to M. Bromley for useful comments on the OPP method, and to G. Gribakin for careful reading of the manuscript and useful comments. This work was supported by the US National Science Foundation under Grants No. PHY-1401788 and PHY-1803744.

---

[1] S. J. Brawley, S. Armitage, J. Beale, D. E. Leslie, A. I. Williams, and G. Laricchia, Science **330**, 789 (2010)

[2] S. J. Brawley, A. I. Williams, M. Shipman, and G. Laricchia Phys. Rev. Lett. **105**, 263401 (2010).

[3] S. J. Brawley, A. I. Williams, M. Shipman, and G. Laricchia, J. Phys.: Conf. Series **388**, 012018 (2012).

[4] M. Shipman, S. J. Brawley, L. Sarkadi, and G. Laricchia, Phys. Rev. A **95**, 032704 (2017).

[5] S. J. Brawley, S. E. Fayer, M. Shipman, and G. Laricchia, Phys. Rev. Lett. **115**, 223201 (2015).

[6] G. Laricchia and H. R. J. Walters, Riv. Nuovo Cimento **35**, 305 (2012).

[7] H. S. W. Massey and H. S. Burhop, Electronic and Ionic Impact Phenomena (Clarendon, Oxford, 1952).

[8] I. I. Fabrikant and G. F. Gribakin, Phys. Rev. Lett. **112**, 243201 (2014).

[9] I. I. Fabrikant and G. F. Gribakin, Phys. Rev. A **90**, 052717 (2014).

[10] G. F. Gribakin, A. R. Swann, R. S. Wilde, and I. I. Fabrikant, J. Phys. B **49**, 064004 (2016).

[11] A. R. Swann and G. F. Gribakin, Phys. Rev. A **97**, 012706 (2018).

[12] J. E. Blackwood, M. T. McAlinden, and H. R. J. Walters, J. Phys. B **35**, 2661 (2002).

[13] M. T. McAlinden, F. G. R. S. MacDonald, and H. R. J. Walters, Can. J. Phys. **74**, 434 (1996).

[14] J. Mitroy and I. A. Ivanov, Phys. Rev. A **65**, 012509 (2001).

[15] J. Mitroy and M. W. J. Bromley, Phys. Rev. A, **67** 034502 (2003).

[16] D. G. Green, A. R. Swann and G. F. Gribakin, Phys. Rev. Lett. **120**, 183402 (2018).

[17] I. I. Fabrikant and R. S. Wilde, Phys. Rev. A **97**, 052707 (2018).

[18] R. S. Wilde and I. I. Fabrikant, Phys. Rev. A **97**, 052708 (2018).

[19] S. Hara, J. Phys. Soc. Jpn., **22**, 710 (1967).

[20] J. K. O'Connell and N. F. Lane, Phys. Rev. A **27**, 1893 (1983).

[21] N. F. Lane, Rev. Mod. Phys. **52**, 29 (1980), p. 47.

[22] E. Wigner and F. Seitz, Phys. Rev. **46**, 509 (1934).

[23] J. C. Slater, Phys. Rev. **81**, 385 (1951).

[24] M. A. Morrison and L. A. Collins, Phys. Rev. A **23**, 127 (1981).

[25] J. Mitroy and G. G. Ryzhikh, Comp. Phys. Comm. **123**, 103 (1999).

[26] I. A. Ivanov, M. W. J. Bromley and J. Mitroy, Comp. Phys. Comm. **152**, 9 (2003).

[27] V. M. Krasnopolsky and V. I. Kukulin, Sov. J. Nucl. Phys. **20**, 883 (1974).

[28] V. I. Kukulin and V. N. Pomerantsev, Ann. Phys. **111**, 330 (1978).

[29] J. B. Mann, At. and Nucl. Data Tables, **12**, 1 (1973).

[30] L. C. Green, M. M. Mulder, M. N. Lewis and J. W. Woll, Phys. Rev. **93**, 757 (1954).

[31] A. R. Swann, J. A. Ludlow, and G. F. Gribakin, Phys. Rev. A **92**, 012505 (2015).

[32] P. A. Fraser, Proc. Phys. Soc. **78**, 329 (1961).

[33] P. A. Fraser, Proc. Phys. Soc. **78**, 721 (1962).

[34] A. Garner, G. Laricchia and A. Ozen, J. Phys. B At. Mol. Phys. **29**, 5961 (1996).

[35] C. Starrett, M. T. McAlinden, and H. R. J. Walters, Phys. Rev. A **72**, 012508 (2005).

[36] M. I. Barker and B. H. Bransden, J. Phys. B **2**, 730 (1969).

[37] O. Hinckelmann and L. Spruch, Phys. Rev. A **3**, 642 (1971).

[38] P. S. Ganas, Phys. Rev. A **5**, 1684 (1972).

[39] I. I. Fabrikant, J. Phys. B **12**, 3599 (1979).

[40] P. A. Fraser, J. Phys. B **1**, 1006 (1968).

[41] M. I. Barker and B. H. Bransden, J. Phys. B **1**, 1109 (1968).

[42] R. J. Drachman and S. K. Houston, J. Phys. B **3**, 1657 (1970).

[43] J. E. Blackwood, C. P. Campbell, M. T. McAlinden and H. R. J. Walters, Phys. Rev. A **60**, 4454 (1999).

[44] P. K. Biswas and S. K. Adhikari, Chem. Phys. Lett. **317**, 129 (2000).

[45] S. K. Adhikari, Phys Rev. A **62**, 062708 (2000).

[46] A. S. Ghosh, A. Basu, T. Mukherjee and P. K. Sinha, Phys. Rev. A **63**, 042706 (2001).

[47] A. Basu, P. K. Sinha and A. S. Ghosh, Phys. Rev. A **63**, 052503 (2001).

[48] S. Chiesa, M. Mella and G. Morosi, Phys. Rev. A **66**, 042502 (2002).

[49] J. DiRenzi and R. J. Drachman, J. Phys. B **36**, 2409 (2003).

[50] H. R. J. Walters, A. C. H. Yu, S. Sahoo and S. Gilmore, Nucl. Instrum. Methods B **221**, 149 (2004).

[51] K. Rytsola, J. Vettenranta, and P. Hautojarvi, J. Phys. B **17**, 3359 (1984).

[52] P. G. Coleman, S. Rayner, F. M Jacobsen, M. Charlton and R. N. West, J. Phys. B **27**, 981 (1994).

[53] K. F. Canter, J. D. McNutt and L. O. Roellig, Phys. Rev. A **12**, 375 (1975).

[54] Y. Nagashima, T. Hyodo, K. Fujiwara and A. Ichimura, J. Phys. B At. Mol. Opt. Phys. **31**, 329 (1998).

[55] Y. Nagashima, T. Hyodo, K. Fujiwara and A. Ichimura, in *The International Conference on the Physics of Electronic and Atomic Collisions, Vancouver, 1995, Abstracts of Contributed Papers* (1995).

[56] M. Skalsey, J. J. Engbrecht, C. M. Nakamura, R. S. Vallery and D. W. Gidley, Phys. Rev. A **67**, 022504 (2003).

[57] J. J. Engbrecht, M. J. Erickson, C. P. Johnson, A. J. Kolan, A. E. Legard, S. P. Lund, M. J. Nyflot and J. D. Paulsen, Phys Rev. A **77**, 012711 (2008).

[58] K. Shibuya and H. Saito, Phys. Rev. A **97**, 052702 (2018).

[59] J. E. Blackwood, M. T. McAlinden and H. R. J. Walters, J. Phys. B **36**, 797 (2003).

[60] Y. Sano, Y. Kino, T. Oka and T. Sekine, J. Phys Conf. Ser. **618**, 012010 (2015).

[61] K. Shibuya, Y. Kawamura and H. Saito, Phys. Rev. A **88**, 042517 (2013).

[62] W. C. Fon, K. A. Berrington, P. G. Burke and H. J. Hibbert, J. Phys. B: At. Mol. Phys. **16**,

307 (1983).

[63] S. J. Buckman and B. Lohmann, J. Phys. B: At. Mol. Phys. **19**, 2547 (1986).

[64] K. Jost, P. G. F. Bisling, F. Eschen, M. Felsmann and L. Walther, *Proc. Int. Conf. Phys. Electron. At. Collisions*, 13 Abstr. p. 91, (1983).

[65] L. T. Sin Fai Lam, J. Phys. B: At. Mol. Phys. **15**, 119 (1982).

[66] M. S. Dababneh, W. E. Kaupilla, J. P. Downing, P. Laperrierr, V. Pol, J. J. Smart and T. S. Stein, Phys. Rev. A **22**, 1872 (1980).

TABLE I: Zero velocity cross sections (in units of 10^{-16} cm^2) and fit parameters (in a.u.) of Eq. (22) for Ps scattering by He and Ne for several correlation models.

Atom, method	$\sigma(v{=}0)$	A	B	C	D
He, FEG	11.04	1.77125	-0.28699	1.02897	-0.71451
He, FEG + Eq. (1), R_c=2.5 a.u.	9.08	1.60567	-0.53912	1.18288	-0.60647
He, FEG, no correlation	12.31	1.87035	0.33931	0	-0.20284
Ne, FEG	12.28	1.86786	-0.33038	1.24721	-0.92570
Ne, FEG+ Eq. (1), R_c=2.5 a.u.	9.09	1.60738	-0.39811	1.23919	-0.89430
Ne, FEG, no correlation	15.21	2.07906	0.642976	0	-0.47386

TABLE II: Zero velocity cross sections (in units of 10^{-16} cm^2) and scattering lengths (in a.u.) of previous calculations and experiments for Ps scattering by He and Ne.

Atom, method	$\sigma(v{=}0)$	A
He, Spherical cavity, frozen target [11]	12.17	1.86
He, Spherical cavity, Eq. (1) R_c=2.5 a.u. [11]	8.13	1.52
He, Spherical cavity, Eq. (1) R_c=3.0 a.u. [11]	9.12	1.61
He, Stochastic variational, frozen target [14]	11.91	1.84
He, Stochastic variational,van der Waals [14]	8.67	1.57
He, Static exchange [40]	12.44	1.88
He, Static exchange [41]	11.40	1.80
He, Static exchange with van der Waals [36]	9.12	1.61
He, Kohn variational, static exchange [42]	10.41	1.72
He, R-matrix, static exchange [43]	12.84	1.91
He, R-matrix, 22 Ps states [43]	11.65	1.82
He, T-matrix, model static exchange [44]	3.73	1.03
He, T-matrix, 3 Ps states, model exchange [45]	2.91	0.91
He, T-matrix, 1 Ps state, 3 He states [46]	6.70	1.39
He, T-matrix, 2 Ps states, 3 He states [46]	6.51	1.36
He, T-matrix, static exchange [47]	13.11	1.93
He, T-matrix, 3 Ps states [47]	12.97	1.92
He, T-matrix, 2 Ps states, 3 He states [47]	6.51	1.36
He, Diffusion Monte Carlo [48]	6.90	1.40
He, Kohn variational, 3 Ps states [49]	9.01	1.60
He, R-matrix, 9 Ps states, 9 He states [50]	9.01	1.6
He, exp. Rytsola *et al.* [51]	7.07	1.42
He, exp. Coleman *et al.* [52]	7.92	1.50
He, exp. Canter *et al.* [53]	7.50	1.46
Ne, Spherical cavity, frozen target [11]	14.36	2.02
Ne, Spherical cavity, Eq. (1) R_c=2.5 a.u [11]	7.50	1.46
Ne, Spherical cavity, Eq. (1) R_c=3.0 a.u [11]	9.70	1.66
Ne, Stochastic variational, frozen target [14]	14.36	2.02
Ne, Stochastic variational, van der Waals [14]	8.45	1.55
Ne, T-matrix, model static exchange [44]	7.00	1.41
Ne, R-matrix, 22 Ps states [12]	14.07	2.0
Ne, exp. Coleman *et al.* [52]	7.92	1.50

TABLE III: Zero velocity cross section in units of (10^{-16} cm^2) and fit parameters of Eq. (22) for Ps scattering by Ar, Kr and Xe using various correlation models.

Atom, correlation model	$\sigma(v{=}0)$	A	B	C	D
Ar, FEG	13.33	1.94669	-0.25754	1.81828	-1.69489
Ar, FEG+Eq. (1), R_c=2.5 a.u.	1.95	0.74374	0.91843	-3.76388	2.81374
Ar, FEG, no correlation	23.86	2.60419	1.64387	0	-1.41846
Kr, FEG	13.86	1.98443	0.25155	1.12354	-1.59459
Kr, Eq. (1), R_c=3.0 a.u.	5.01	1.19382	0.94039	-3.44121	2.42489
Kr, no correlation	28.41	2.84166	2.07948	0	-1.81308
Xe, FEG	12.14	1.85763	5.02004	-10.4840	6.05051
Xe, Eq. (1), R_c=3.0 a.u.	8.06	-1.51357	-14.14210	18.6610	-6.80718
Xe, no correlation	35.21	3.16358	3.45205	0	-3.63689

TABLE IV: Zero velocity cross sections (in units of 10^{-16} cm^2) and scattering lengths (in a.u.) of previous calculations and experiments for Ps scattering by Ar, Kr and Xe.

Atom, correlation model	$\sigma(v{=}0)$	A
Ar, spherical cavity, frozen target [11]	27.78	2.81
Ar, spherical cavity, Eq. (1) R_c=2.5 a.u [11]	7.20	1.43
Ar, spherical cavity, Eq. (1) R_c=3.0 a.u [11]	16.42	2.16
Ar, stochastic variational, frozen target [14]	28.58	2.85
Ar, stochastic variational, van der Waals [14]	8.45	1.55
Ar, Pseudopotential, static exchange [9]	35.81	3.19
Ar, Pseudopotential, Eq. (1) R_c=2.5 a.u. [9]	16.11	2.14
Ar, Pseudopotential, Eq. (1) R_c=3.0 a.u. [9]	19.10	2.33
Ar, T-matrix, model static exchange [44]	9.58	1.65
Ar, R-matrix, 22 Ps states [12]	14.07	2.0
Ar, exp. Coleman *et al.* [52]	7.92	1.50
Kr, spherical cavity, frozen target [11]	34.03	3.11
Kr, spherical cavity, Eq. (1) R_c=3.0 a.u [11]	17.97	2.26
Kr, spherical cavity, Eq. (1) R_c=3.5 a.u [11]	23.06	2.56
Kr, stochastic variational, frozen target [14]	35.58	3.18
Kr, stochastic variational, van der Waals [14]	13.79	1.98
Kr, Pseudopotential, static exchange [9]	38.78	3.32
Kr, Pseudopotential, Eq. (1) R_c=3.0 a.u. [9]	19.43	2.35
Kr, Pseudopotential, Eq. (1) R_c=3.5 a.u. [9]	21.99	2.50
Kr, R-matrix, static exchange [12]	38.32	3.3
Xe, spherical cavity, frozen target [11]	46.88	3.65
Xe, spherical cavity, Eq. (1) R_c=3.0 a.u [11]	24.34	2.63
Xe, spherical cavity, Eq. (1) R_c=3.5 a.u [11]	29.18	2.88
Xe, stochastic variational, frozen target [14]	51.34	3.82
Xe, stochastic variational, van der Waals [14]	18.45	2.29
Xe, Pseudopotential, static exchange [10]	35.81	3.19
Xe, Pseudopotential, Eq. (1) R_c=3.0 a.u. [10]	21.12	2.45
Xe, R-matrix, static exchange [59]	50.00	3.77
Xe, exp. Shibuya and Saito [58]	14.93	2.06

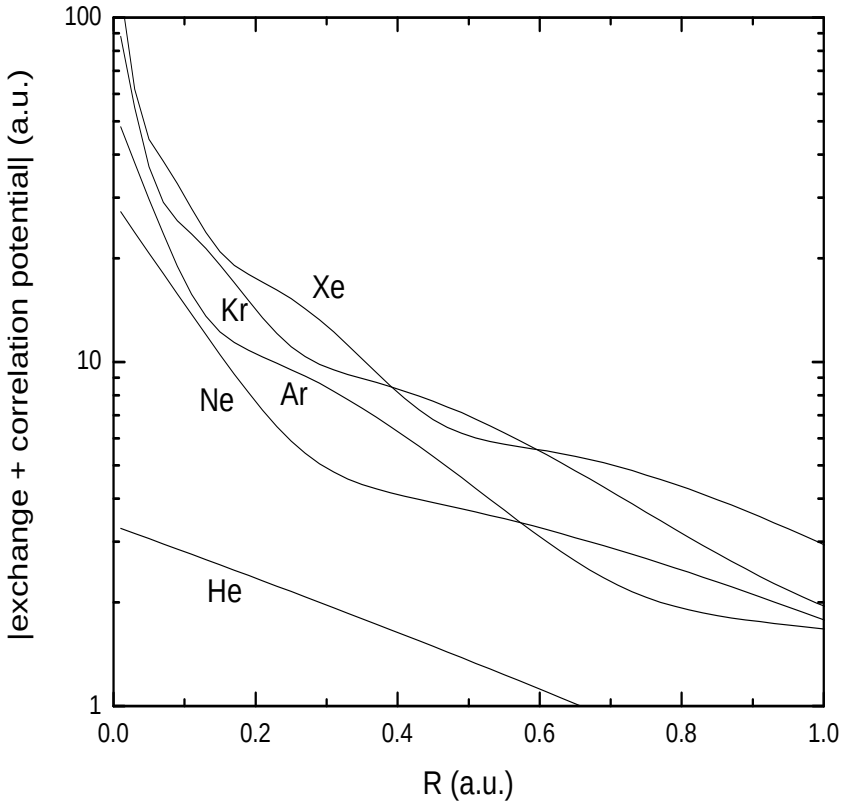

FIG. 1: Absolute value of the FEG exchange plus correlation potential for Ps-Rg scattering as a function of Ps center of mass R at small values of R.

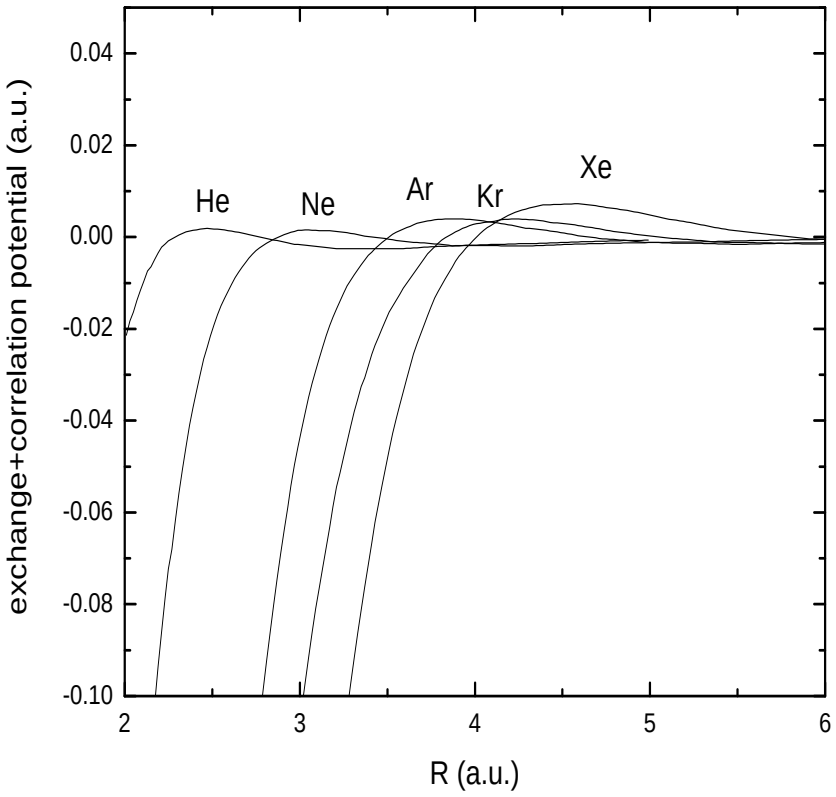

FIG. 2: FEG exchange plus correlation potentials for Ps-Rg scattering as a function of the position R of the Ps center of mass at intermediate values of R.

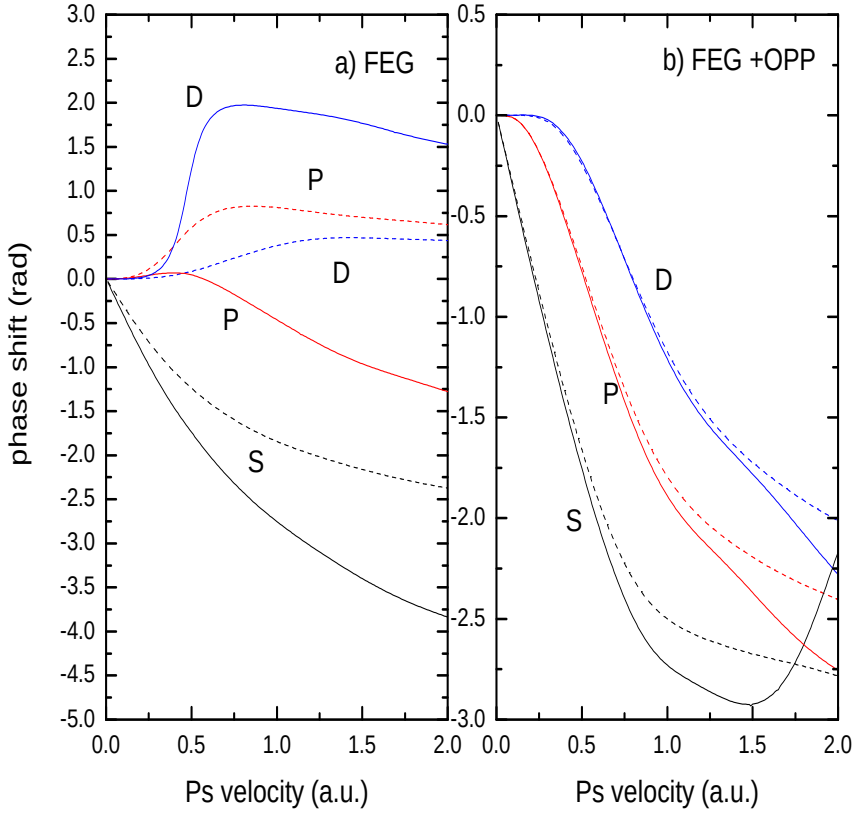

FIG. 3: Phase shifts for Ps scattering by Helium and Neon using a) FEG exchange and correlation potentials and b) FEG exchange and correlation plus OPP. Solid lines: Neon; Dashed lines: Helium. Black lines: S wave, red lines: P wave, blue lines: D wave.

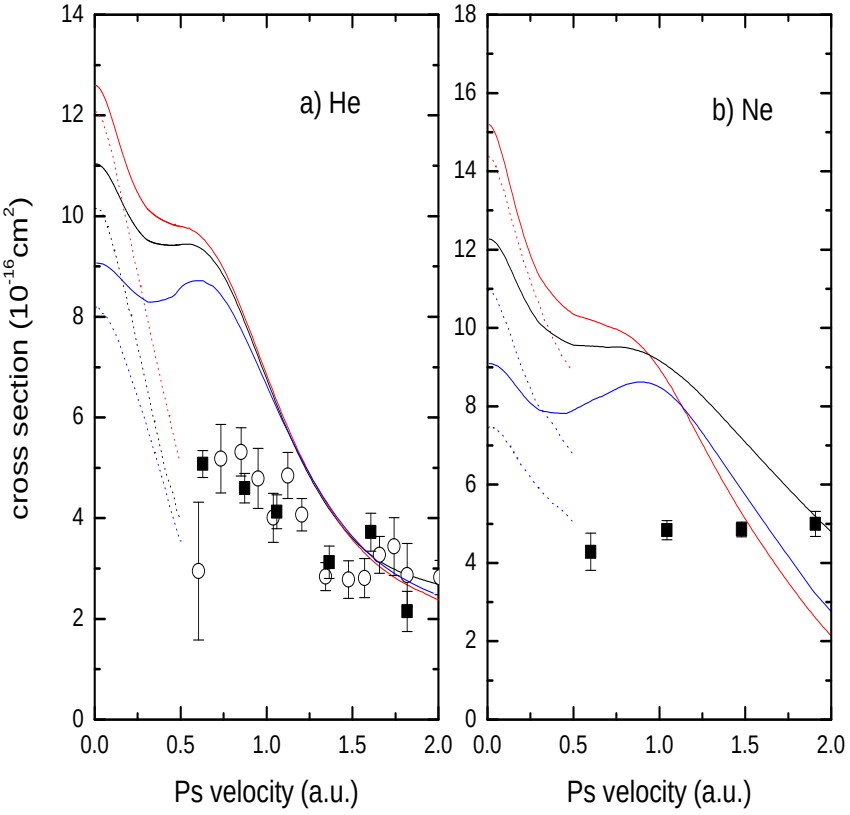

FIG. 4: Cross sections for Ps scattering by a) Helium and b) Neon. Black solid lines (middle curve at v=0): elastic cross section using local FEG exchange and correlation potentials with OPP. Red solid lines (upper curve at v=0): elastic cross section using only the local FEG exchange potential plus OPP. Blue solid lines (lower curve at v=0): elastic cross section using the local FEG exchange potential and correlation potential of Eq. (1) with a cutoff radius of R_c=2.5 a.u. Dashed line (middle curve): Many body theory results of [16]. Red dashed lines (upper curve): frozen target calculations of [11]. Blue dashed lines (lower curve): calculations of [11] using the correlation potential of Eq. (1) with a cutoff radius of R_c=2.5 a.u. Squares: total cross section measurements of [1]. Circles: total cross section measurements of [34].

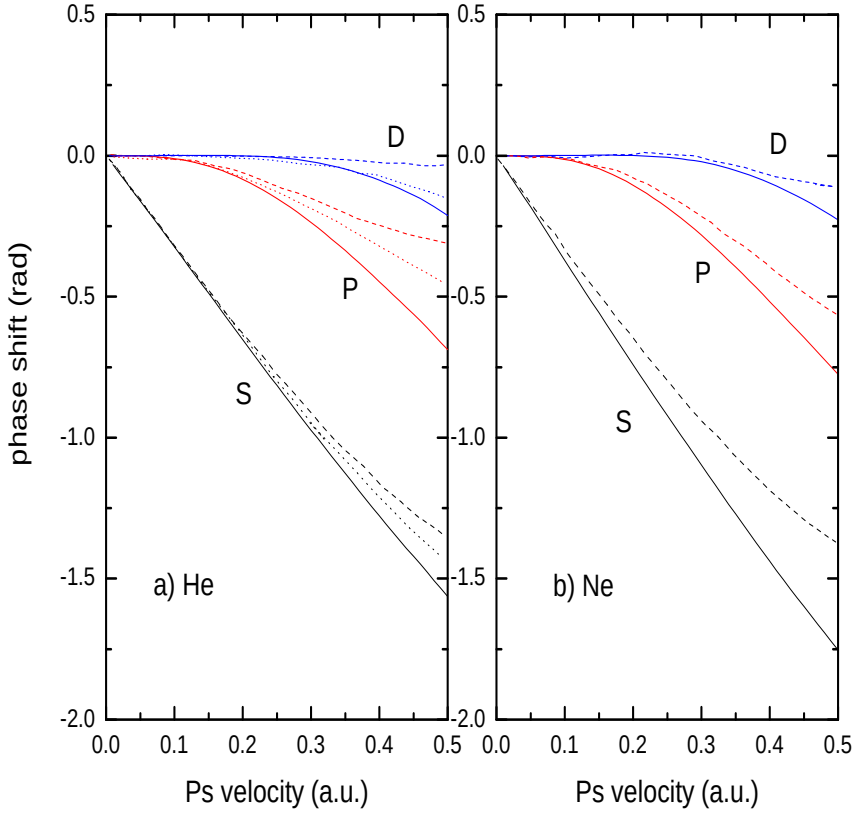

FIG. 5: Phase shifts for Ps scattering by a) Helium and b) Neon using the FEG exchange potential plus the OPP and correlation potential of Eq. (1) with a cutoff radius of R_c=2.5 a.u. Black lines: S wave, red lines: P wave, blue lines: D wave. Solid lines: present results; dashed lines: results of ref [11] using the same correlation potential; dotted lines: results of Barker and Bransden [36].

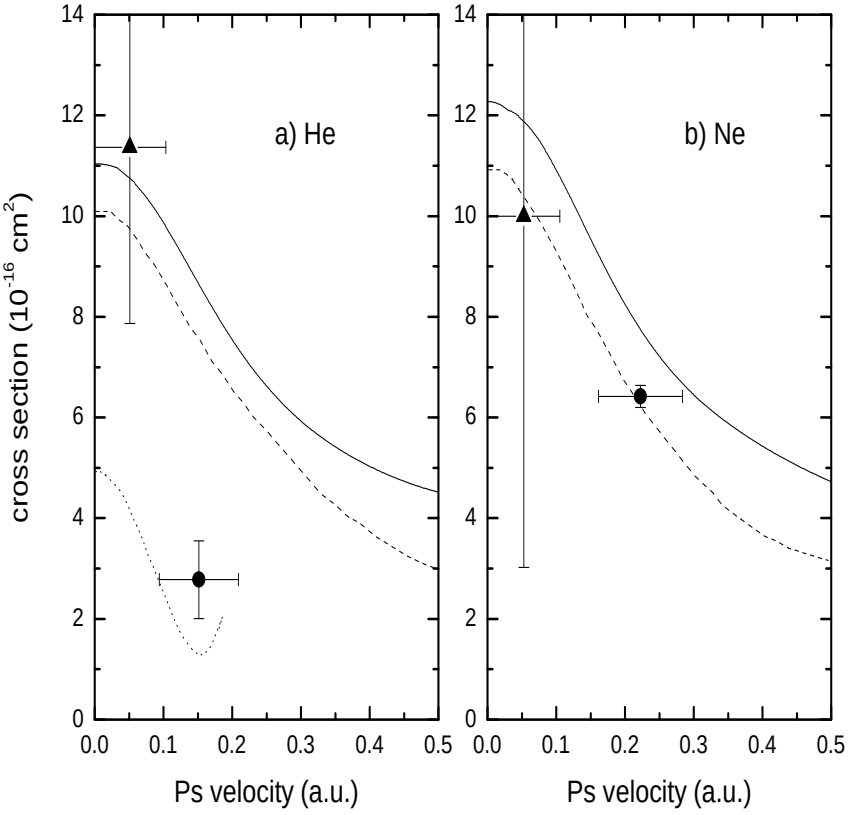

FIG. 6: Momentum transfer cross sections for Ps scattering by a) He and b) Ne. Solid lines: present FEG plus OPP results. Dashed lines: many body theory calculations of [16]. Experimental results, Triangle: Nagashima *et al.* [54, 55], Circles: Skalsey *et al.* [56], dotted line: Engbrecht *et al.* [57].

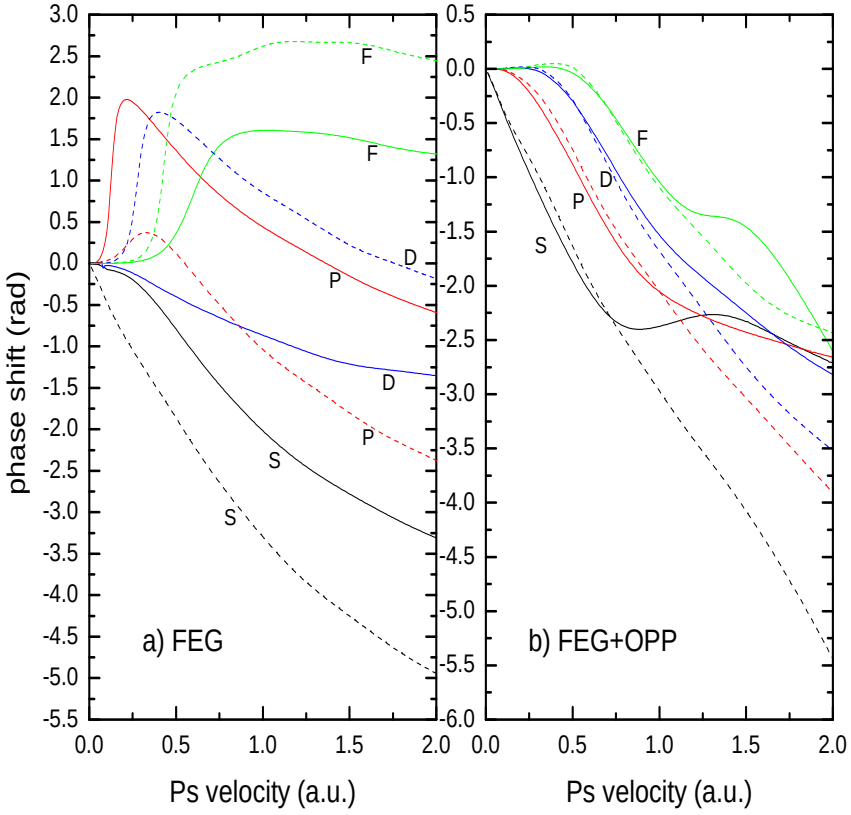

FIG. 7: Phase shifts for Ps scattering by Argon and Xenon using a) FEG exchange and correlation potentials and b) FEG exchange and correlation plus OPP. Solid lines: Argon; Dashed lines: Xenon. Black lines: S wave, red lines: P wave, blue lines: D wave, green lines: F wave.

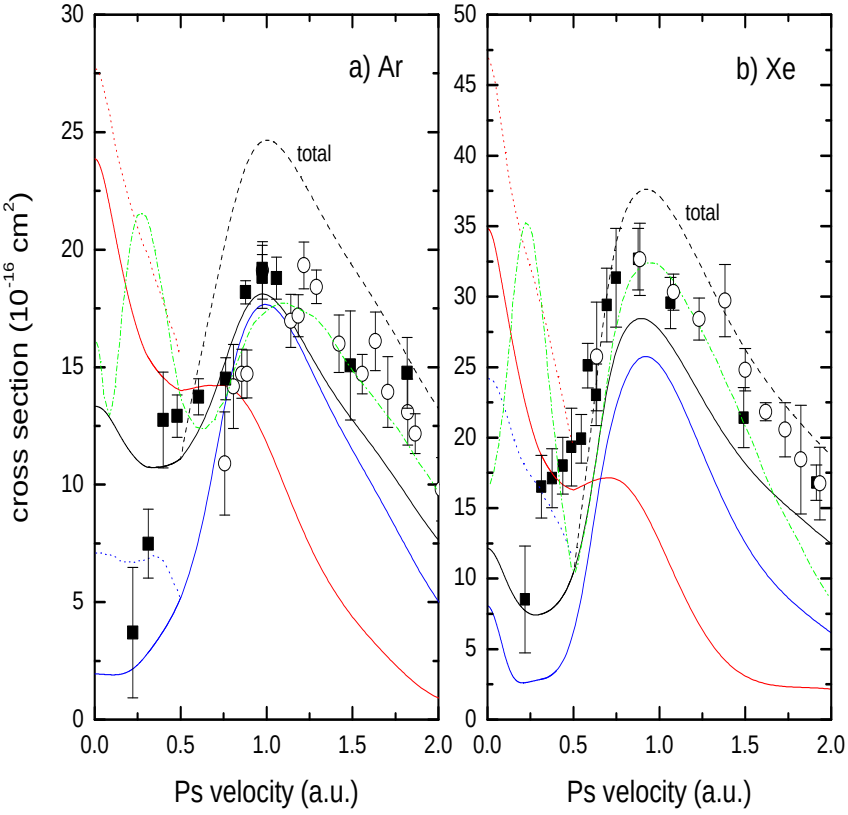

FIG. 8: Cross sections for Ps scattering by a) Argon and b) Xenon. Solid lines (middle curves at $v = 0$): elastic cross section using local FEG exchange and correlation potentials with OPP. Dashed line (labeled total): total cross section (elastic plus ionization) Red solid lines (upper curves at v=0): elastic cross section using only the local FEG exchange potential plus OPP. Blue solid lines (lower curves at v=0): elastic cross section using the local FEG exchange potential plus OPP and correlation potential of Eq. (1) with a cutoff radius of R_c=2.5 a.u. for Ar and R_c = 3.0 a.u. for Xe. Green dot-dash lines: total cross sections of the pseudopotential method [10]. Red dotted lines (upper curves): frozen target calculations of [11]. Blue dotted lines (lower curves): calculations of [11] using the correlation potential of Eq. (1) with a cutoff radius of R_c=2.5 a.u. for Ar and R_c=3.0 for Xe. Circles: total cross section measurements of [1]. Squares: total cross section measurements of [5].

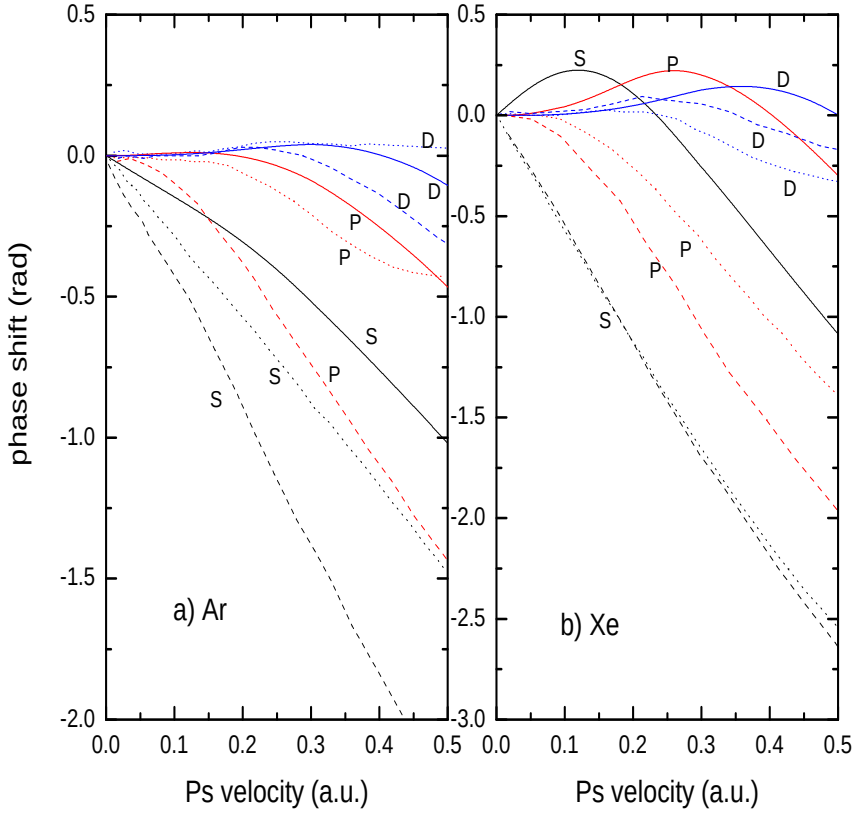

FIG. 9: Phase shifts for Ps scattering by a) Argon and b) Xenon using the FEG exchange potential plus the OPP and correlation potential of Eq. (1) with a cutoff radius of R_c=2.5 a.u. for Argon and R_c= 3.0 for Xenon. Black lines: S wave, red lines: P wave, blue lines: D wave. Solid lines: present results; dashed lines: pseudopotential results of ref [10]; dotted lines: results of ref. [11].

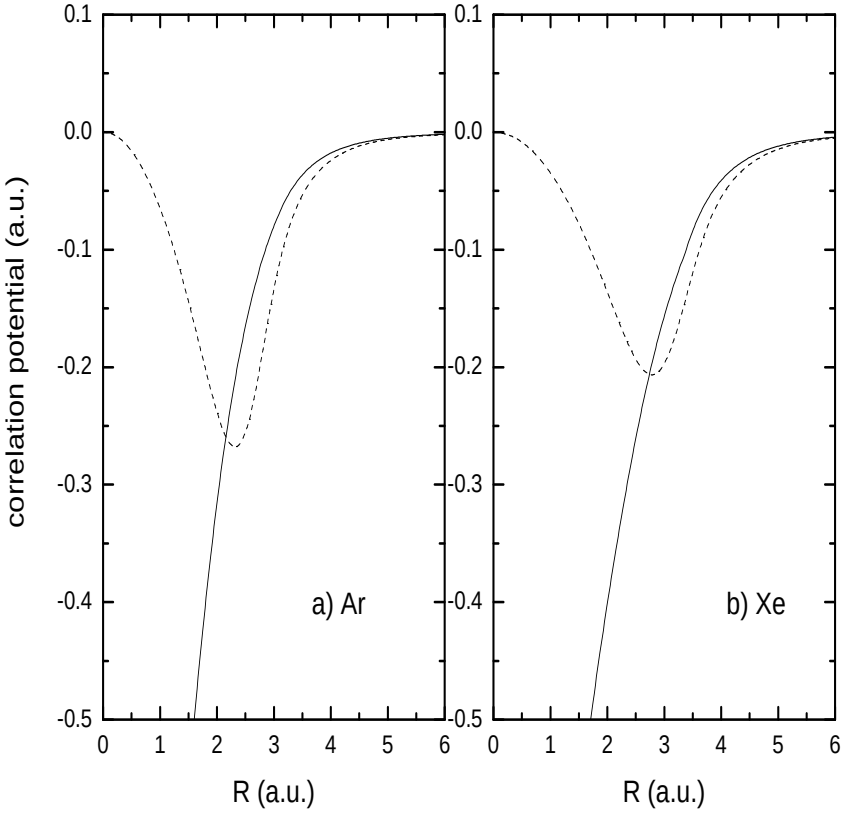

FIG. 10: Correlation potentials for a) Argon and b) Xenon. Solid line: FEG correlation potential. Dashed line: Correlation with cutoff potential of (1) with R_c=2.5 a.u. for Ar and 3.0 a.u. for Xe.

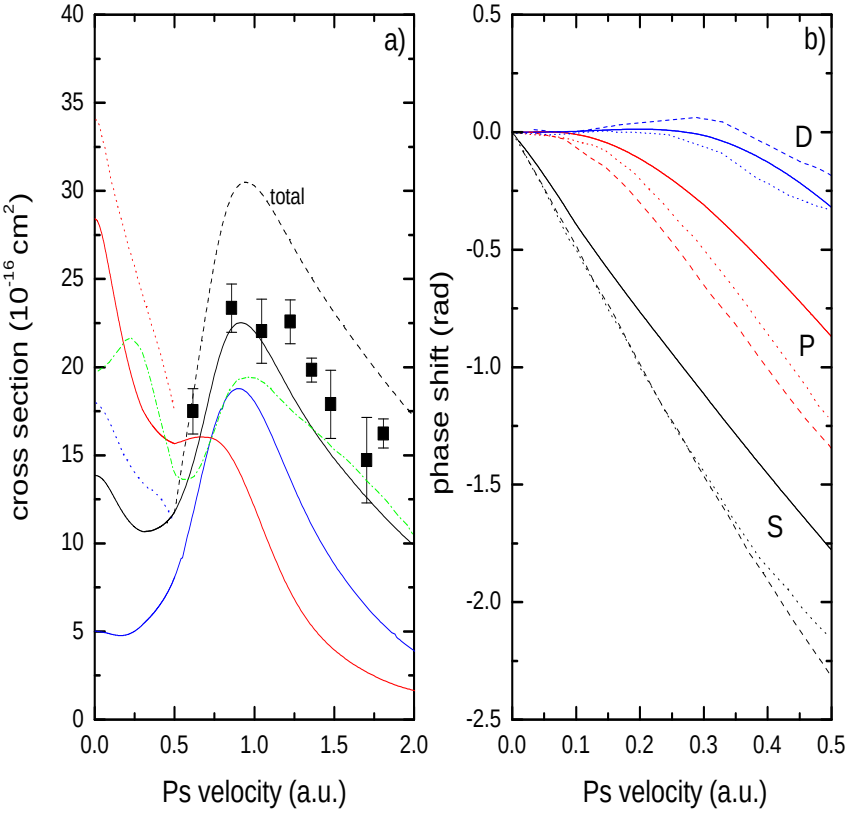

FIG. 11: Cross sections and phase shifts for Ps scattering by Kr. a) Solid line (middle curve at v=0): elastic cross section using local FEG exchange and correlation potentials with OPP. Dashed line (labeled total): total cross section (elastic plus ionization). Red solid line (upper curve at v=0): elastic cross section using only the local FEG exchange potential plus OPP. Blue solid line (lower curve): elastic cross section using the local FEG exchange potential plus OPP and correlation potential of Eq. (1) with a cutoff radius R_c = 3.0 a.u. Red dotted line (upper curve): frozen target calculations of [11]. Blue dotted line (lower curve): calculations of [11] using the correlation potential of Eq. (1) with a cutoff radius of R_c=3.0 a.u. Green dash-dot line: pseudopotential results of [10]. Squares: total cross section measurements of [1]. b)Phase shifts for Ps-Kr using local FEG exchange and correlation potentials with OPP. Black line: S wave, red line: P wave, blue line: D wave. Dashed lines are pseudopotential phase shifts of [10] and dotted lines are phase shifts of [11] with the correlation potential of Eq. (1) with a cutoff radius of R_c=3.0 a.u.

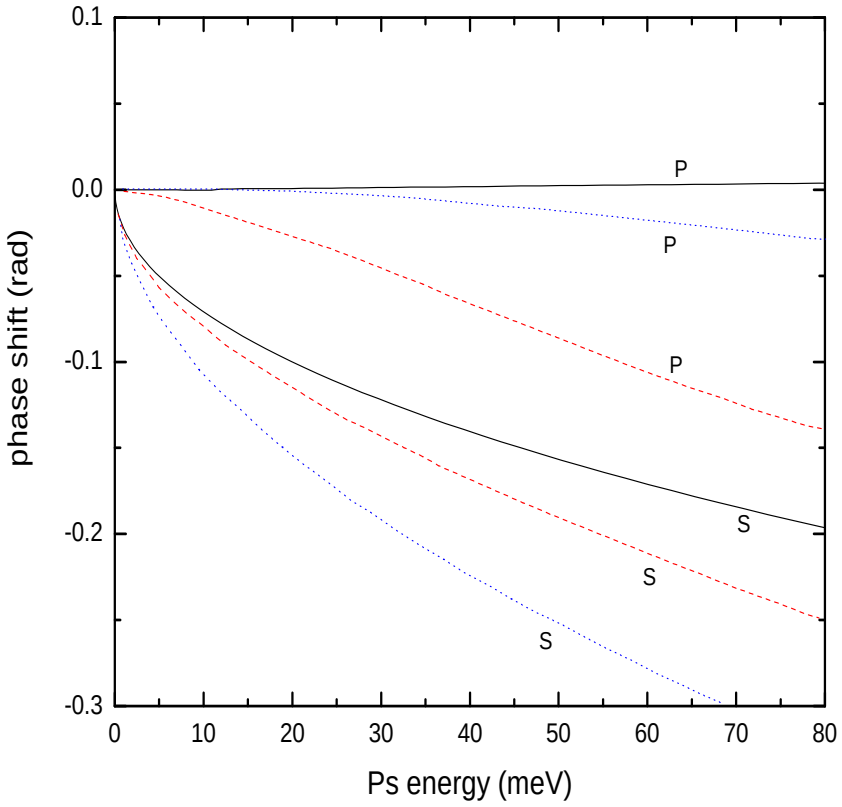

FIG. 12: S- and P-wave phase shifts for Ps-Xe scattering at low Ps energies. Solid lines: Present FEG+OPP results. Dashed red lines: Shibuya and Saito [58]. Dotted blue lines: pseudopotential results [10].

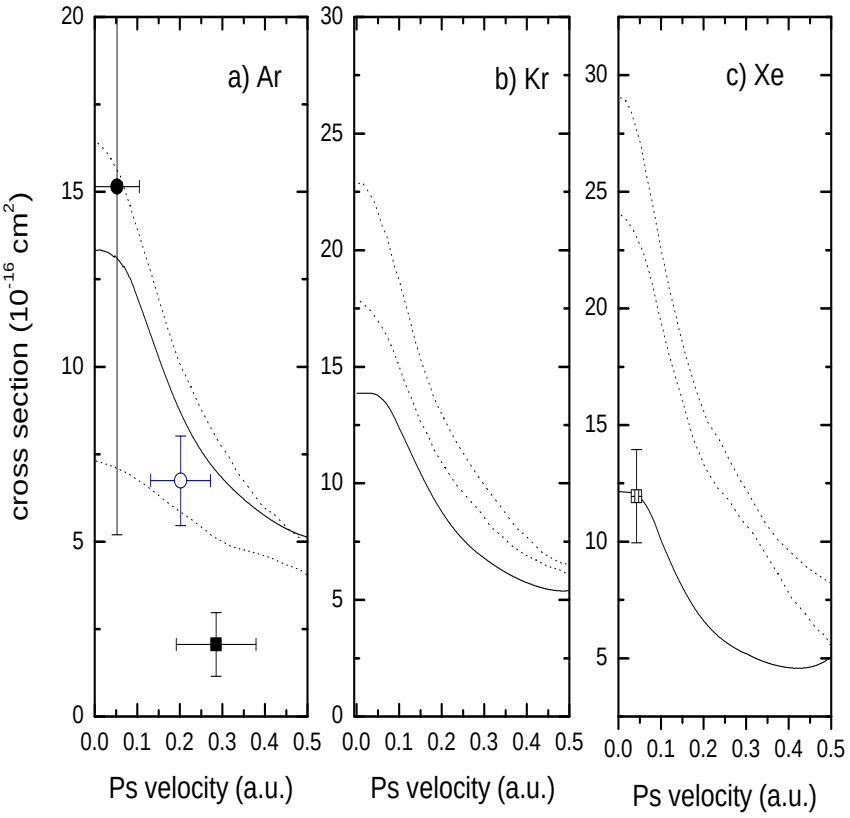

FIG. 13: Momentum transfer cross sections for heavy rare gas atoms. Solid lines: present calculations using FEG exchange and correlation potentials plus the OPP. Dotted lines: calculations of [11] with correlation potential of Eq. (1), larger cross sections are using $R_c = 3.0$ a.u. for Ar and 3.5 a.u. for Kr and Xe while smaller cross sections are using $R_c = 2.5$ a.u. for Ar and 3.0 a.u. for Kr and Xe. Experimental results for Ar, closed circle: Nagashima *et al.* [55]; open circle: Skalsey *et al.* [56]; closed square: Sano *et al.* [60]. Experimental result for Xe, open square: Shibuya *et al.* [61].

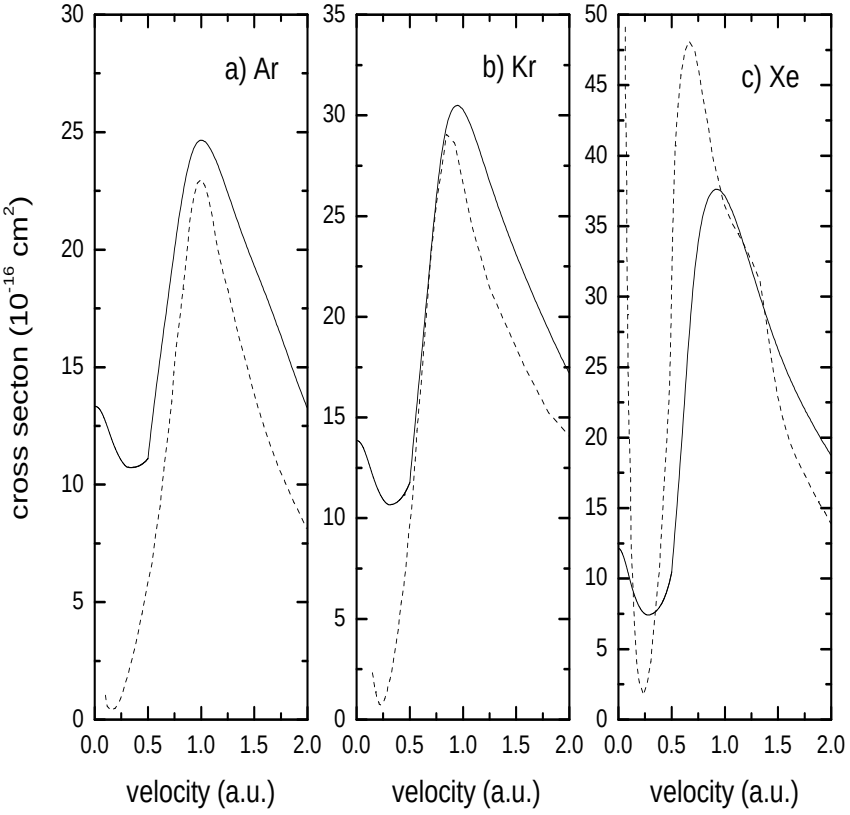

FIG. 14: Comparison of Ps scattering and electron scattering cross sections for a) Ar, b) Kr and c) Xe. Solid lines: present Ps total (elastic plus ionization) cross sections with local FEG exchange and correlation potentials plus OPP. Dashed lines: total electron scattering cross sections, for Ar compiled from the calculations [62] and measurements [63], for Kr measurements [64] and for Xe compiled from calculations [65] and measurements [66].